

# Solar arch filaments observed with THEMIS\*

P. Mein<sup>1</sup>, C. Briand<sup>2,1</sup>, P. Heinzel<sup>3</sup>, and N. Mein<sup>1</sup>

<sup>1</sup> Observatoire de Paris, Section de Meudon, DASOP-LPSH, UMR 8645, 92195 Meudon Cedex, France

<sup>2</sup> Themis, IAC, Via Lactea, 38205 La Laguna, Tenerife, Spain

<sup>3</sup> Astronomical Institute, Academy of Sciences of the Czech Republic, 25165 Ondřejov, Czech Republic

Received 28 September 1999 / Accepted 22 December 1999

**Abstract.** Arch Filaments (AF) have been observed in the Ca II 8542 Å line with the THEMIS telescope in September 1998. We present a preliminary analysis of MSDP spectro-imaging data. A cloud-model fit provides line-of-sight velocities and a set of plausible values for the model parameters. The high sensitivity of the filament opacity to temperature, coupled with the rough linearity versus electronic density, shows that this Ca II line should be very efficient to complement usual H $\alpha$  data for a more rigorous diagnostics.

**Key words:** Sun: chromosphere – Sun: filaments – line: profiles

## 1. Introduction

Arch Filament Systems (AFS) have been extensively studied in the H $\alpha$  line (Bruzek 1969; Alissandrakis et al. 1990; Tsiropoula et al. 1992; Chou 1993). Material flows along the legs were compared to free fall motions (Schmieder et al. 1991). The upward velocities at the top of the arches were used as an indicator of magnetic field emergence into the low corona (Mein P. et al. 1996). When simultaneous X-ray data were available, the association between AFS and coronal loops was investigated and sheared magnetic topologies were derived (Malherbe et al. 1998).

However, a full analysis of thermodynamical conditions was not made so far. One of the reasons is that the AFS are observable only in a few visible lines. The aim of this paper is to show that the Ca II lines, which are sensitive to collisional processes, are good indicators of the electronic temperatures and densities.

In two previous papers, we have studied the formation of the hydrogen H $\alpha$  line inside a moving plasma cloud, located above the solar surface and illuminated by solar radiation (see Mein N. et al. 1996; Heinzel et al. 1999). For such clouds, Molowny-Horas et al. (1999) have developed an inversion technique to derive the cloud velocity and basic plasma parameters. However, the reliability of such spectroscopic diagnostics is substantially enhanced if other spectral lines of other chemical species are

used. Therefore, a new program of detecting the Ca II IR line at 8542 Å has been recently initiated, using the MSDP installed at THEMIS telescope. The first MSDP spectroimaging data, which are described in this paper, were obtained in 1998. They provide line profiles both in the AFS and in the surrounding chromosphere and thus are well suited for application on cloud models.

## 2. Spectro-imaging data: THEMIS and the MSDP spectrographs

THEMIS is a 90 cm-aperture telescope, especially designed for high spatial resolution and polarization measurements. Spectroscopy in many lines, narrow band filtergrams and subtractive imaging spectroscopy are available. For more details on the THEMIS capabilities see <http://www.obs-nice.fr/themis>. We shall only mention briefly the Multichannel Subtractive Double Pass spectrograph which produced the data analysed in this paper.

The principle is similar to that of other MSDPs in operation, such as the MSDP attached to the German VTT at the Teide Observatory (Mein 1991). However, two improvements must be pointed out. The first one is the use of two different gratings for the two passes in order to reduce the scattered light. The second one is the use of new “beamshifters” allowing for higher spectral resolutions (Mein 1995).

The Ca II 8542 Å profiles are observed simultaneously in 16 wavelengths (same atmospheric effects at all wavelengths), in a field of view of 75” $\times$ 8”. The local bandpass is about 62 mÅ, and the distance between channels is 125 mÅ in the case of Ca II 8542. The detectors are 2 CCD cameras (288 $\times$ 384 pixels of 0.34” $\times$ 0.34”), each camera recording 8 channels. By joining overlapping spectro-images, full maps can be computed over large fields of view (scanning step 5”).

The delay between two successive exposures is roughly 2 s with an integration time of 300 ms.

## 3. Ca II line profiles of arch filaments

The MSDP data were obtained on September 10, 1998, on the active region NOAA 8331 (N25 E30,  $\mu \simeq 0.8$ ).

The THEMIS data are processed in the following way:

*Send offprint requests to:* P. Mein (meinp@obspm.fr)

\* Based on observations made with the THEMIS telescope operated on the island of Tenerife by CNRS-CNR in the spanish Observatorio del Teide of the Instituto de Astrofísica de Canarias

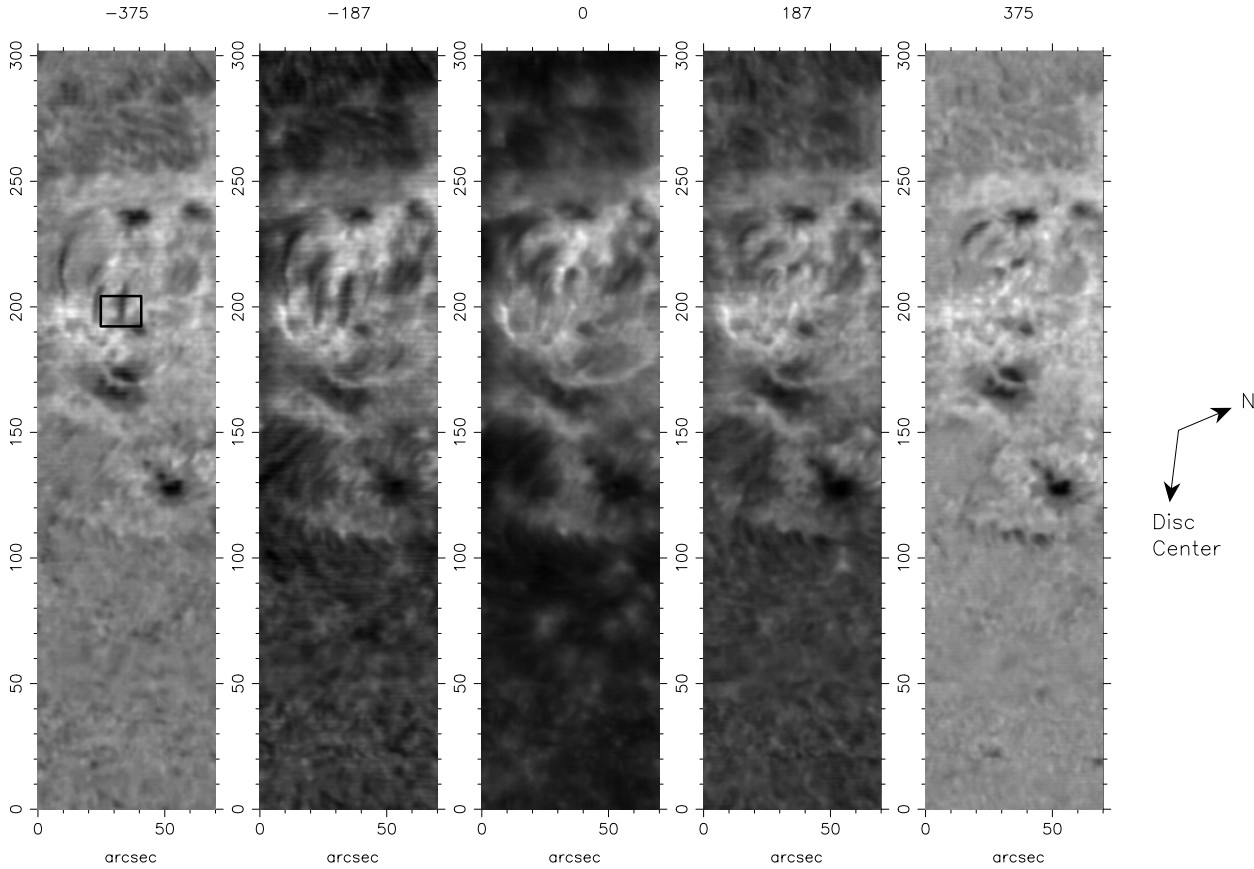


**Fig. 1.** Filtergrams of Ca II 8542 deduced from MSDP THEMIS data. Wavelengths with respect to line center are mentioned at the top in mÅ. The black rectangle ( $16'' \times 12''$ ) in the left-hand map corresponds to the range of line profiles shown in Fig. 2. AF analysed in this paper is seen in the middle of this rectangle.

- the accurate positions of the MSDP channels are computed in each image (edges of the channels determined by the use of thresholds and maximum signal gradients); new files are computed by spatial interpolation with a pixel of  $0.25''$  (smaller than the observing pixel to preserve the spatial resolution);

- all images are corrected for dark current and flat field;
- line profiles in each point of the field of view are derived from the 16 channels and interpolated by spline functions.

An overview of the reduction process can be found in Roudier et al. (1991). More details, concerning the different corrections used in this processing, will be given later in a paper devoted to the instrument itself.

Fig. 1 shows computed maps of line profile intensities around 16:50 UT, for 5 wavelengths between  $-375$  and  $375$  mÅ. The total field of view is  $70'' \times 300''$ .

Sunspots are clearly visible in the line wings. Bodies of arch filaments are seen both in the line center and in the blue wing, because of strong velocities. Perspective effects enhance the blueshifts for material moving upwards and towards the disc center.

The full lines of Fig. 2 present a series of profiles corresponding to the small rectangle shown in Fig. 1. The wavelength range is  $\pm 0.43$  Å. The dashed lines represent the quiet sun profile averaged over the lower part of the field of view (Fig. 1).

The distance between two successive plots is  $2''$ . We see an absorbing and blueshifted AF from profiles (0,3) to (0,-2). To the top left (-4,3), we see a part of another filament. In the bottom right corner, dark profiles indicate the vicinity of a small spot (4,-3).

Cloud models are well suited for the analysis of AFS and imaging spectroscopy facilitates the choice of neighbouring points, showing the underlying chromosphere.

The central profile (0,0) is in the body of one of the arch filaments and will be analysed in this paper.

#### 4. Ca II 8542 Å line formation in a dynamical cloud model

In this section we discuss a potential diagnostics of Ca II 8542 line, in the frame of the cloud-model approach previously used for hydrogen  $H\alpha$  line. Following problems are to be addressed: Calcium atomic model, cloud geometry and boundary conditions (incident radiation).

##### 4.1. Calcium atomic model

Based on results of Gouttebroze et al. (1997), we use here a 5-level Ca II atom plus continuum. We neglect Ca I which is much less populated compared to calcium ions. Ca III dominates Ca II

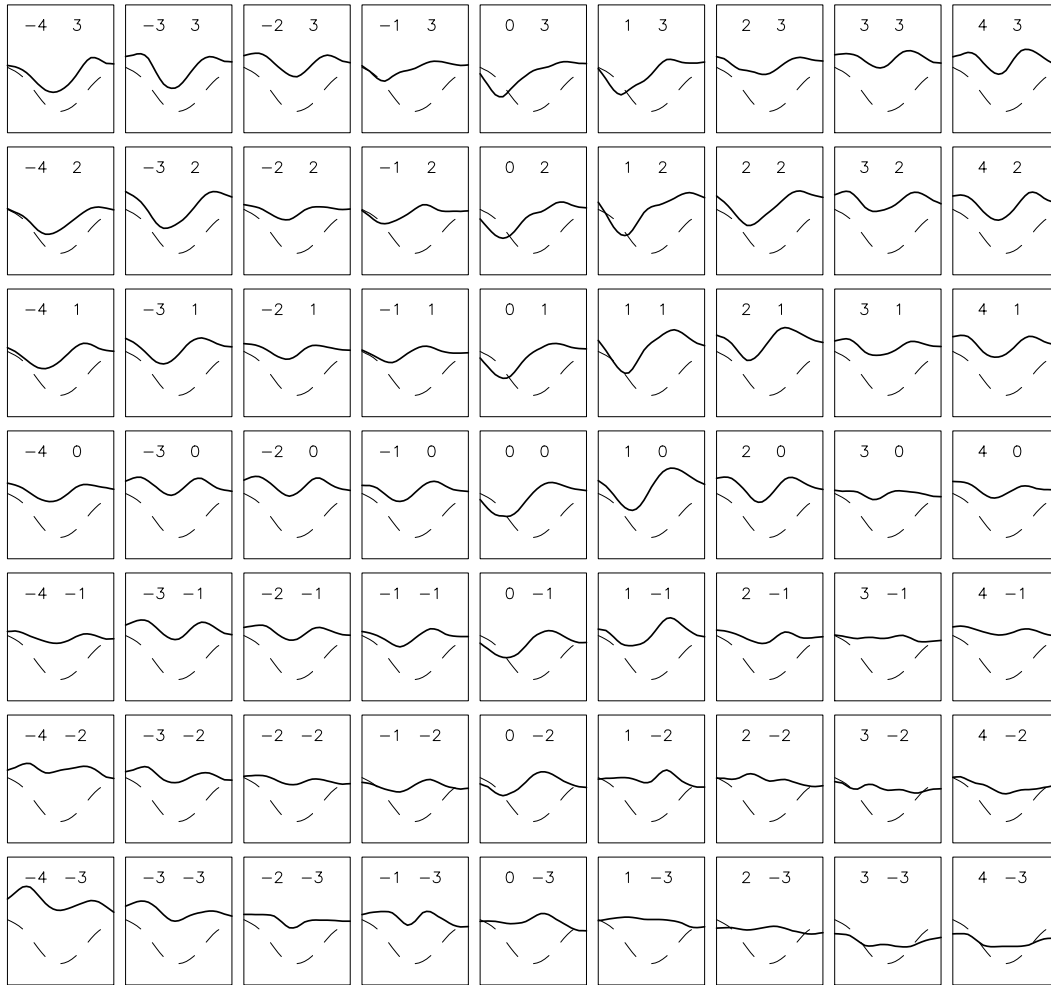


**Fig. 2.** Ca II 8542 profiles corresponding to the range of the rectangle noted in Fig. 1 (index unit  $2''$ ). The profile (0,0) is used as typical AF profile, and the average of (-2,0) and (2,0) as chromospheric profile below the filament. Dashed lines show the quiet sun profile.

at temperatures higher than 6000 K. Ca II atomic-level structure, transition rates, level-broadening parameters and photoionization cross-sections are the same as summarized by Shine & Linsky (1974). The Ca II 8542 Å infrared line results from the transition between the levels  $4p^2P_{3/2}$  and  $3d^2D_{5/2}$ . A special attention is deserved to the evaluation of photoionization rates. We consider five continuum transitions, the resonance continuum at 1044 Å, and four subordinate continua at 1218, 1219, 1417 and 1422 Å. At these wavelengths, the photoionization by the hydrogen Lyman lines and continuum radiation fields is important, as already noted by Ishizawa (1971). Here we follow the procedure used by Gouttebroze et al. (1997), assuming that all these continua are optically thin and thus their photoionization rates are fixed by the radiation fields inside the cloud (we have verified this assumption for typical cloud-model conditions). First, the radiation field in the Lyman lines and continuum is computed by solving the NLTE problem for hydrogen (as in Heinzel et al. 1999), and the depth-dependent mean intensities are stored. They are subsequently used in the calcium code to evaluate the photoionization rates, which contain also the contribution from other frequency ranges where the internal field is fixed by the diluted incident solar radiation. The latter is taken from UV observations.

#### 4.2. Cloud geometry and incident radiation

For the purposes of this paper we use the same 1D cloud geometry as in Mein N. et al. (1996) and Heinzel et al. (1999). This is certainly a great simplification. However, we try first to understand the physics of 8542 Å line formation in clouds which was not studied before in this way. Only later on we shall improve the modelling by using a 2D approach similar to that of Paletou (1995), but including the macroscopic cloud velocities in analogy to present 1D case.

For the Ca II photoionization, the geometry is less important since we assume optically-thin continuum transitions (although the internal hydrogen radiation fields depend on the true geometry). For the five lines we solve the transfer equation with the incident radiation compiled from various solar observations (same data were used in Gouttebroze et al. 1997).

The NLTE problem of calcium excitation and ionization balance is solved using the MALI (Multilevel Accelerated Lambda Iteration) technique, in the same way as in the case of hydrogen (Heinzel et al. 1999). This also includes the effects of macroscopic velocities. Partial-redistribution effects on the level populations are approximated by restricting the resonance-lines frequency range to three Doppler widths and by using the complete

frequency redistribution (CRD). Infrared lines are computed with CRD.

Finally, once the opacity and the source function for the studied line are known, we perform the formal solution of the transfer equation *along the line of sight*, taking into account the Doppler shift (due to the projected velocity vector) and the observed background radiation as the lower boundary condition. The resulting profile shows a typical absorption shifted due to cloud motion. This intensity profile is a combination of the background intensity attenuated by the cloud plus the cloud emission. For clouds which are optically thick in Ca II 8542 Å line, the shift of the absorption profile gives directly the line-of-sight velocity. However, under typical cloud conditions, this line is not thick and thus a detailed NLTE solution is required to infer the true velocity.

### 5. Model of a typical arch filament

We analyse the profile of the AF shown in the central part of Fig. 2 (profile 0,0). The geometrical thickness  $D$  of the filament can be estimated from Fig. 1. There is negligible perspective effect because the filament is pointing to disc centre. The width is around 3". By assuming a cylindrical shape, we get roughly  $D = 2200$  km.

To estimate the chromospheric background below the AF along the line-of-sight, we average two profiles at  $\pm 5''$  from the AF. On Fig. 2, they correspond to profiles in between (-2,0) and (-3,0) for the first one, and (2,0) and (3,0) for the second one.

We present in Fig. 3 the observed AF profile of Ca II 8542 Å (full line), the chromospheric background profile (dashed line) and the reference quiet sun profile (dotted line).

The incident radiation depends on the altitude of the AF (assumed to be 5000 km) and the brightness of the underlying chromosphere. The ratio between the quiet sun profile and the background profile is around 3 at the line center and 1 in the wings. We approximate the incident radiation by the quiet sun illumination multiplied by a factor  $\alpha = 2$ .

The crosses in Fig. 3 show the theoretical profile obtained with the following optimal model parameters:

- temperature  $T = 8000$  K
- electronic density  $N_e = 0.6 \times 10^{11} \text{ cm}^{-3}$
- microturbulence  $\xi = 5 \text{ km s}^{-1}$
- line-of-sight velocity  $v = 12 \text{ km s}^{-1}$ , corresponding to an upward velocity of  $15 \text{ km s}^{-1}$
- geometrical thickness  $D = 2200$  km
- incident radiation factor  $\alpha = 2$

$v$  and  $\xi$  are mainly determined by the shift and the width of the AF profile.  $N_e$  corresponds to typical values for AFS (Malherbe et al. 1998).  $T$  is adjusted to get a good fit with the data.

The discrepancy around the wavelength  $0.0 \text{ \AA}$  cannot be reduced, because the intensity of the absorbing AF cannot exceed the background intensity. This points out the difficulty to

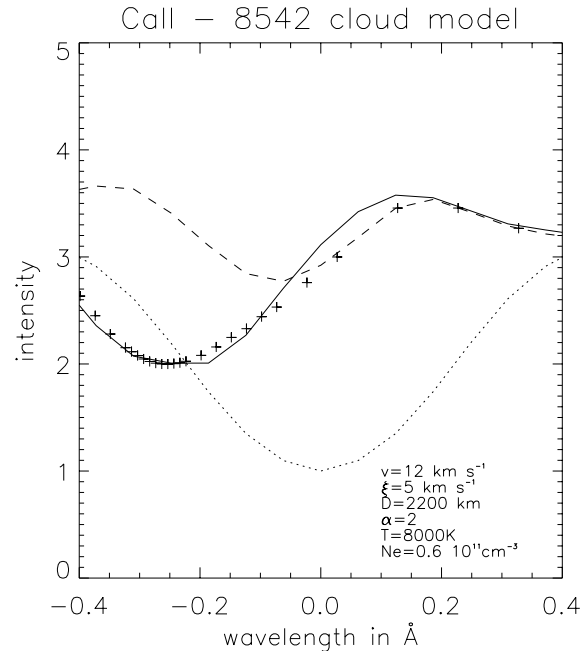


**Fig. 3.** Fitting of the observed profile. Full line: observed profile, crosses: calculated profile with  $v=12 \text{ km s}^{-1}$ ,  $\xi = 5 \text{ km s}^{-1}$ ,  $D=2200$  km,  $T=8000$  K,  $N_e=0.6 \cdot 10^{11} \text{ km s}^{-1}$ , dotted line: quiet chromosphere, dashed line: background profile. The intensities are normalized to the center of the quiet sun profile.

eliminate the fluctuations of the background radiation. Since we cannot assume a constant source function throughout the AF, we cannot use the technique of “differential” cloud model (Mein & Mein 1988).

### 6. Sensitivity of line profiles to model parameters

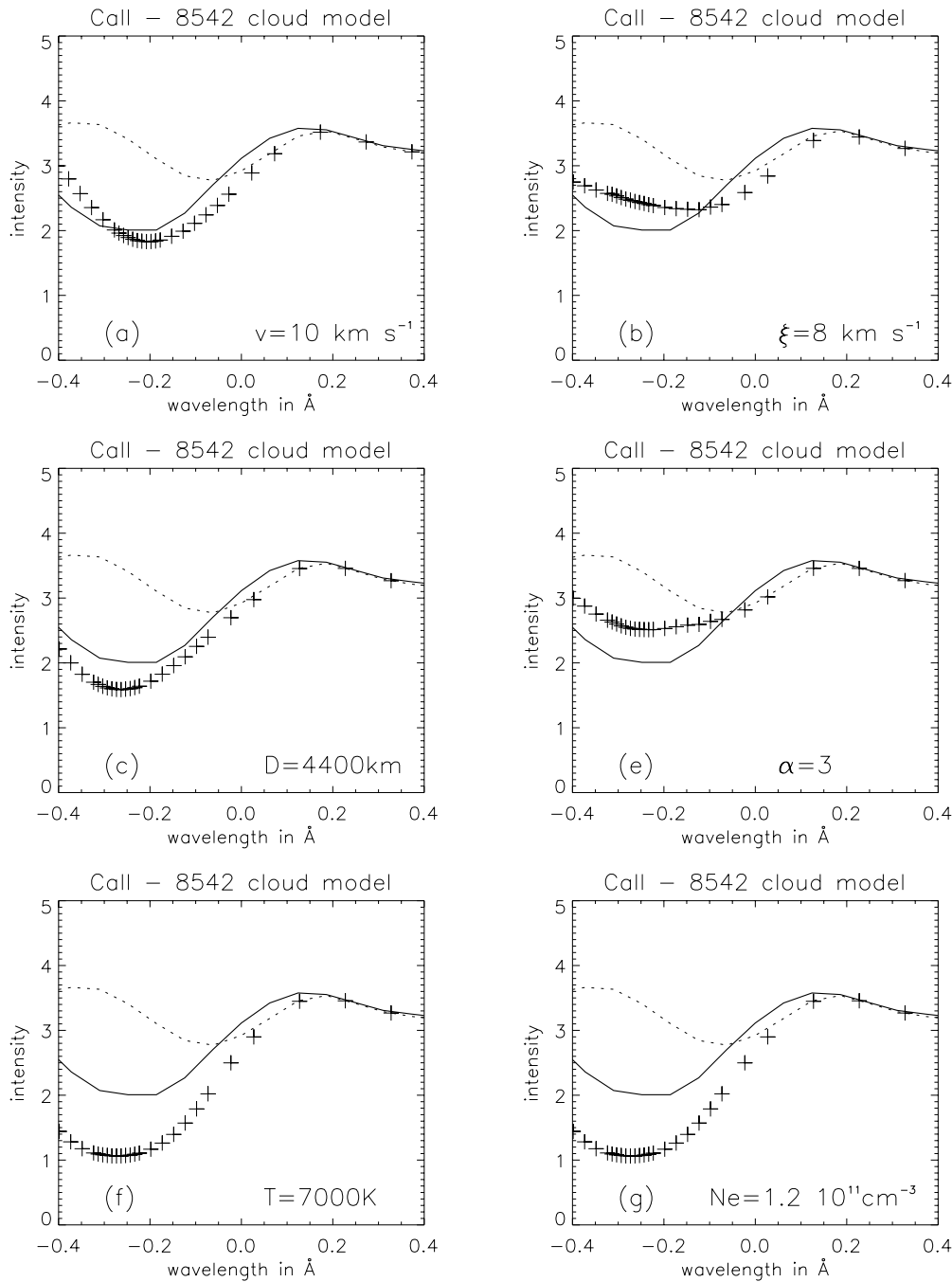
Although a more detailed analysis is required to specify the sensitivity of the profiles to the model parameters, we can determine some trends around the values mentioned above.

Fig. 4 presents the theoretical profiles obtained successively by modifying  $v$ ,  $\xi$ ,  $D$ ,  $\alpha$ ,  $T$  and  $N_e$ . The results show that the accuracy of the fit is better than 1 and 2  $\text{km s}^{-1}$  for  $v$  and  $\xi$ , respectively.

It is interesting to compare the opacity fluctuations of the AF when changing  $D$ ,  $\alpha$ ,  $T$  or  $N_e$ . The line-center optical thickness of the theoretical AF is 0.9 in the fitted model. It becomes 1.5 for  $h = 4400$  km, 0.8 for  $\alpha = 3$ , 4.3 for  $T = 7000$  K and 2.0 for  $N_e = 1.2 \times 10^{11} \text{ cm}^{-3}$ . This shows that, *around the fitted model*, the opacity increase is slower than that of  $D$ , and is approximately proportional to  $N_e$  (and not to  $N_e^2$  as for H $\alpha$ , see Heinzel et al. 1994). Moreover, the sensitivity to temperature is very high (more than a factor of 4 for a decrease of 1000 K). The sensibility to  $\alpha$  is not very high.

### 7. Conclusions

We have analysed THEMIS/MSDP data obtained in 1998 to investigate the structure and dynamics of a peculiar arch filament.



**Fig. 4.** Sensitivity to the different parameters around the solution shown in Fig. 3. The modified values are printed in each case. Full line: observed profile, crosses: calculated profile, dashed line: background profile.

A dynamical cloud model based on the MALI code was used to fit the line profile of Ca II 8542 Å. Line-of-sight velocity and microturbulence are well determined. Sensitivities to the geometrical thickness, temperature and electronic density seem to be different from those known for the H $\alpha$  line, which suggests a useful complementary diagnostics.

As a next step, it would be interesting to obtain observations in H $\alpha$  and Ca II 8542 *simultaneously*. This will be possible using the MSDP on THEMIS. Both profiles should then be analysed by using a 2D dynamical cloud model. Inversion with a grid of models (see Molowny-Horas et al. 1999) can be also used since the grid dimensions depend more on the number of parameters

than on the number of line profiles. Such inversion methods are very promising (namely using more lines), however, to construct a grid of 2D models would be very time-consuming.

*Acknowledgements.* We want to take the opportunity of this paper, which is the first obtained with the MSDP mode of THEMIS, to thank all the people involved in the THEMIS project. In particular, we are extremely grateful to J. Rayrole who has been the leader for the project development. We thank all the THEMIS team for the efficient help during the observing campaign. PH acknowledges the support of Observatoire de Meudon and of the grant K1-003-601 of the Academy of Sciences of the Czech Republic.

**References**

- Alissandrakis C.E., Tsiropoula G., Mein P., 1990, A&A 230, 200
- Bruzek A., 1969, Solar Phys. 8, 29
- Chou D.Y., 1993, In: Zirin H., Ai P., Wang H. (eds.) ASP conf. series vol. 46, p. 471
- Gouttebroze P., Vial J.-C., Heinzel P., 1997, Solar Phys. 172, 125
- Heinzel P., Gouttebroze P., Vial J.-C., 1994, A&A 292, 656
- Heinzel P., Mein N., Mein P., 1999, A&A 346, 322
- Ishizawa T., 1971, PASJ 23, 75
- Malherbe J.M., Schmieder B., Mein P., et al., 1998, Solar Phys. 180, 265
- Mein N., Mein P., Heinzel P., et al., 1996, A&A 309, 275
- Mein P., 1991, A&A 248, 669
- Mein P., 1995, In: Comte G., Marcelin M. (eds.) ASP conf. series vol. 71, p. 350
- Mein P., Mein N., 1988, A&A 203, 162
- Mein P., Démoulin P., Mein N., et al., 1996, A&A 305, 343
- Molowny-Horas R., Heinzel P., Mein P., Mein N., 1999, A&A 345, 618
- Paletou F., 1995, A&A 302, 587
- Roudier T., Mein P., Muller R., et al., 1991, A&A 248, 237
- Shine R.A., Linsky J.L., 1974, Solar Phys. 39, 49
- Schmieder B., Raadu M.A., Wiik J.E., 1991, A&A 252, 353
- Tsiropoula G., Georgakilas A.A., Alissandrakis C.E., Mein P., 1992, A&A 262, 587